Journal of Alloys and Compounds 509 (2011) 8676–8682

Contents lists available at ScienceDirect

Journal of Alloys and Compounds

journal homepage: www.elsevier.com/locate/jallcom

Realization of stable p-type ZnO thin films using Li–N dual acceptors

T. Prasada Rao, M.C. Santhosh Kumar*

Advanced Materials Laboratory, Department of Physics, National Institute of Technology, Tiruchirappalli- 620 015, India

ARTICLE INFO

Article history:
Received 6 January 2011
Received in revised form 19 May 2011
Accepted 24 May 2011
Available online 23 June 2011

PACS:
68.37.Ps
68.55.J
73.61.Ga
78.20.Ci

Keywords:
p-ZnO
Structural properties
Strain
Electrical resistivity
Optical properties

ABSTRACT

Lithium and nitrogen dual acceptors-doped p-type ZnO thin films have been prepared using spray pyrolysis technique. The influence of dual acceptor (Li, N) doping on the structural, electrical, and optical properties of (Li, N):ZnO films are investigated in detail. The (Li, N):ZnO films exhibit good crystallinity with a preferred *c*-axis orientation. From AFM studies, it is found that the surface roughness of the thin films increases with the increase of doping percentage. The Hall Effect measurements showed p-type conductivity. The Hall measurements have been performed periodically up to seven months and it is observed that the films show p-type conductivity throughout the period of observation. The samples with Li:N ratio of 8:8 mol% showed the lowest resistivity of 35.78 Ω cm, while sample with Li:N ratio of 6:6 mol% showed highest carrier concentration. The PL spectra of (Li, N):ZnO films show a strong UV emission at room temperature. Furthermore, PL spectra show low intensity in deep level transition, indicating a low density of native defects. This indicates that the formation of intrinsic defects is effectively suppressed by dual acceptor (Li, N) doping in ZnO thin films. The chemical bonding states of N and Li in the films were examined by XPS analysis.

1. Introduction

Zinc oxide (ZnO) is a subject of current interest, because of its potential applications in optoelectronic devices, transparent electrodes and window materials for displays and solar cells. Since, it is a wide band gap (3.37 eV at room temperature) semiconductor with a large exciton binding energy (about 60 meV). For the development of ZnO based devices, it is necessary to have p- and n-type ZnO. However, the lack of good and reliable p-type ZnO has been a major problem for many years, due to the asymmetric doping limitations in ZnO [1]. Mandel [2] suggested that the resistance to form p-type doping is because of the "self-compensation" of shallow acceptors resulting from various naturally occurring or spontaneously generated donor defects such as oxygen vacancies (V_O) or zinc vacancies or interstitials (Zn_i). In order to achieve p-type conduction in ZnO, these donors like native defects have to be suppressed or even eliminated. According to theory, Li and N are the best two candidates in producing p-type ZnO based on their strain effects and energy levels of substitutional Li_{Zn} and N_O acceptors [3]. Unfortunately, these dopants can easily form donor levels in ZnO, such as Li interstitials (Li_i) in ZnO:Li and N_2-on-O substitutions [$(N_2)_O$] in ZnO:N [4,5] leading to self-compensations, which is the main difficulty in producing p-type ZnO. Yamamoto et al. [6] proposed a codoping method using acceptors (N) and donors (Ga, Al, In) simultaneously in order to increase the solubility of nitrogen concentration in ZnO thin films. Several codoping methods have been reported to prepare the p-type ZnO thin films by different donors, such as Ga, Al, and In [7–9]. But they also face the self-compensation effect, since donor dopants are introduced into ZnO. Hence, such p-type ZnO thin films are poor in reproducibility. Lu et al. [10] demonstrated that the Li–N dual-acceptor doping method, which is very promising in producing low-resistivity; stable p-type ZnO thin films.

In the present investigation, p-type ZnO thin films are deposited by Spray Pyrolysis technique via a dual-acceptor doping method. The dual-acceptors namely nitrogen and lithium are simultaneously introduced in the samples during deposition. Structural, electrical and optical properties of these films are investigated.

2. Experimental

The precursor solution for spray pyrolysis was prepared by dissolving appropriate amounts of zinc acetate dihydrate in a mixture of deionized water and ethanol at room temperature. In this mixture, ethanol concentration was 10 ml in 100 ml solution. Aqueous solutions of ammonium acetate and lithium acetate were used as dopant sources for N and Li, respectively. A few drops of acetic acid were added to aqueous solutions to prevent the formation of hydroxides. The total concentration of the solution was maintained at 0.3 mol L^{-1}. Four different sets of thin films were deposited with Li:N = 2:2, 4:4, 6:6 and 8:8 mol%. Dual acceptor doped ZnO thin films were deposited on glass substrates at a substrate temperature of 623 K. The glass

* Corresponding author. Tel.: +914312503611.
E-mail addresses: prasadview@gmail.com (T.P. Rao), santhoshmc@nitt.edu, santhoshmc@yahoo.com (M.C.S. Kumar).

0925-8388/$ – see front matter © 2011 Elsevier B.V. All rights reserved.
doi:10.1016/j.jallcom.2011.05.094

substrates were cleaned thoroughly with acetone, isopropanol, deionized water and finally cleaned with the help of an ultrasonic bath for 30 min and dried. The spray nozzle was at a distance of 20 cm from the substrate during deposition. The solution flow rate was held constant at 3 ml/min. Air was used as the carrier gas at the pressure of 2 bar.

The structural characterization was carried out by X-ray diffraction (XRD) measurements using Rigaku D/Max ULTIMA III diffractometer with CuK_α radiation ($\lambda = 1.5406$ Å). The average dimensions of crystallites were determined by the Scherer method from the broadening of the diffraction peaks. The surface morphology profiles of the samples were recorded using Nanoscope-E instrument in contact mode with a Si_3N_4 cantilever of atomic force microscope (AFM). Electrical properties namely, resistivity, Hall mobility, and carrier concentration were measured at room temperature using Ecopia Hall measurement system (Model: HMS-3000) in van der Pauw configuration. The X-ray photoelectron spectroscopy (XPS) data were recorded at a base pressure of 3×10^{-10} mbar using an AlKα laboratory X-ray source that was operated at 100 W and a commercial electron energy analyzer with five channeltrons from Specs GmbH, Germany. The thickness of the samples was measured using Stylus profile meter and it is found that the average film thickness is 550 nm for all samples.

3. Results and discussion

3.1. Structural characteristics

XRD pattern of the (Li, N):ZnO films were recorded in the range of 2θ between 20° and 60°. Fig. 1 shows the XRD patterns of the as-prepared (Li, N):ZnO thin films with different Li and N concentrations. All the films show the existence of a very strong peak corresponding to (002) and weak peaks corresponding to (100), (101) reflections of the wurtzite phase of ZnO. The strong and dominating nature of the peak corresponding to the (002) reflection indicates the preferential *c*-axis orientation of crystallites. The *c* axis orientation in (Li, N):ZnO films can be understood from the "survival of the fastest" model proposed by Van der Drift [11]. According to this model, nucleations with various orientations can be formed at the initial stage of the deposition and each nucleus competes to grow but only nuclei having the fastest growth rate can survive. Also, the (002) orientated grains are reported to have the lowest surface energy [12]. The diffraction peaks are easily indexed on the basis of the hexagonal structure of ZnO ($a = 3.242$ Å, and $c = 5.194$ Å, JCPDS 75-0576). Moreover, the intensity of the (002) peak found to decrease significantly with increase of Li and N mol% content in the films. The decreasing tendency in intensity of (002) peak indicates that the incorporation of lithium and nitrogen in to ZnO films with the same film thickness of 550 nm [13]. This behaviour indicates that the increase in the doping concentration deteriorates the crystallinity of the films, which may be attributed to the influence of stresses arising from the incorporation of Li and N [14]. It is also observed that the full width at half maximum (FWHM) of the peak corresponding to the (002) reflection is found to increase with Li and N incorporation in the films. In addition to this the (002) peaks showed a slight deviation from ($2\theta = 34.50°$) the value for ZnO powder (JCPDS 75-0576). A marginal deviation was observed for as deposited (Li, N):ZnO films as shown in Table 1. In addition to this for the (Li, N):ZnO films, both the intensity and full width at half-maximum (FWHM) of diffraction peaks are sensitive to the dual acceptor doping. These deviations indicate a variation in interplanar spacing relative to that of the ZnO powder, which is probably due to the factors such as lattice strain and interstitial defects. Scherer's formula was employed to estimate the grain size of (Li, N):ZnO films, given by

$$D = \frac{0.9}{\beta \cos\ \theta} \quad (1)$$

where D is the average dimension of the grains normal to the reflecting planes, β is the crystallite-size breadth defined by $\beta^2 = B^2 - b^2$, in which B is the FWHM of observed peak and b is

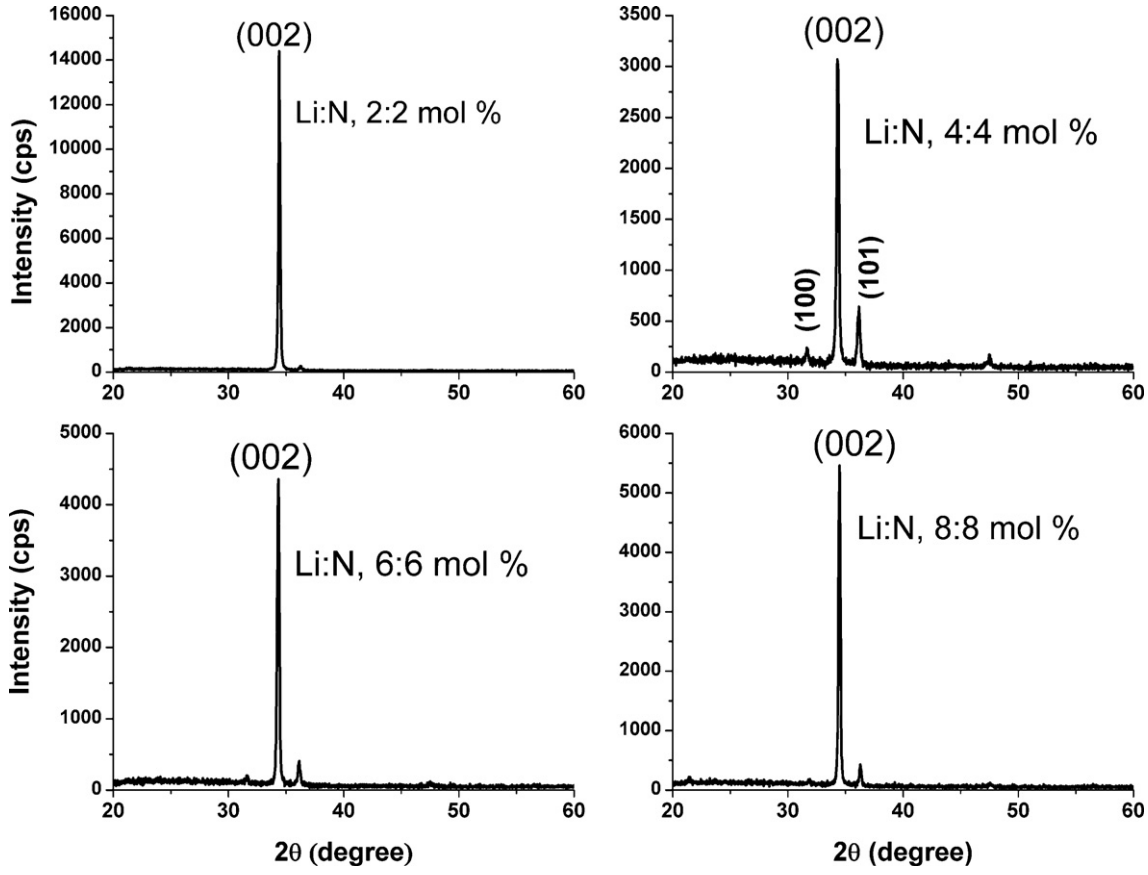

Fig. 1. XRD patterns of (Li, N):ZnO films.

Table 1
Lattice constants, FWHM, grainsize, rms roughness, strain and stress of (Li, N):ZnO films.

Li (mol%)	N (mol%)	c (Å)	2θ (degree)	FWHM (degree)	Grain size (nm) XRD	Particle size (nm) AFM	Roughness (nm)	Strain (%)	Stress (GPa)
2	2	5.1987	34.476	0.1719	48.39	223.72	55.23	0.090	−0.410
4	4	5.2010	34.460	0.1577	52.71	158.14	62.17	0.134	−0.611
6	6	5.2198	34.332	0.1993	41.72	131.03	71.44	0.496	−2.253
8	8	5.2213	34.322	0.1859	44.71	232.46	79.55	0.525	−2.384

the instrumental factor. Table 1 shows the variations of full-width at half-maximum (FWHM), position of (0 0 2) peak and grain size. It can be seen from the data that as dopant concentration increases the FWHM increases, while the grain size decreases. The reduction in the ZnO grain growth may be due to the reduction in concentration of the zinc interstitials. When Li and N concentration increases in ZnO films, the concentration of zinc interstitials decrease because of the charge compensation process in the sample. The lattice constant 'c' as calculated for (0 0 2) plane using the following equation [15]:

$$\frac{1}{d^2_{(hkl)}} = \frac{4}{3}\left[\frac{h^2 + hk + k^2}{a^2}\right] + \frac{l^2}{c^2} \quad (2)$$

These values are found to be larger than that of bulk ZnO value of 0.5194 nm (JCPDS-75-0576). This indicates that the films have residual tensile strain along the c-axis [16]. The average uniform strain ε_{zz} in the lattice along the c-axis of the ZnO films have been estimated from the lattice parameters using the following expression [15]:

$$\varepsilon_{zz} = \frac{(c - c_0)}{c_0} \times 100\% \quad (3)$$

where c_0 is the unstrained lattice parameter of ZnO. The residual stress in the films is composed of thermal stress and intrinsic stress. The former comes from the difference in the thermal expansion coefficients between the coating and the substrate, while the latter originates from the in grown defects or structural mismatch between the film and substrate [17]. In this study, the dependence of total residual stress on the incorporation on dual acceptor was investigated, with the assumption that thermal stress is a constant, since the deposition temperature maintained constant for all samples. For hexagonal crystals, the stress (σ) in the plane of the film can be calculated using the biaxial strain model [18]:

$$\sigma_{\text{film}} = \frac{2C_{13}^2 - C_{33}(C_{11} + C_{12})}{C_{13}}\varepsilon_{zz} \quad (4)$$

where C_{11} = 209.7 GPa, C_{12} = 121.1 GPa, C_{13} = 105.1 GPa, and C_{33} = 210.9 GPa are the elastic stiffness constants of bulk ZnO. Calculated grain size, lattice parameter, strain and stress are shown in Table 1. The value of σ is negative, demonstrating that the stresses in the deposited films are compressive in the direction of the c-axis. It is well known fact that defects in the films are formed during the growth process. These defects cause lattice disorder, which generates the intrinsic stress in the films. From Table 1, it has been proved that, under the present deposition conditions, the Li and N elements promote a growth with the c axis perpendicular to the substrate.

The surface morphology of the thin films was investigated by atomic force microscopy (AFM). The scanning area was 5 μm × 5 μm (3- dimensional images) and 1 μm × 1 μm. The AFM images of the (Li, N):ZnO thin films are shown in Fig. 2. The values of particle size and root mean square (rms) roughness obtained from AFM are listed in Table 1. From the table, it is observed that the measured size of the particle from the AFM surface images is higher than the values calculated from XRD studies, indicating that these particles are probably an aggregation of small crystallites on the surface of the films. However, XRD is giving average size of the crystallites. The variation in values of surface roughness increases with increase in doping concentration.

3.2. Electrical properties

The electrical properties of as-deposited films were investigated by Hall-effect measurement in van der Pauw configuration at room temperature. Table 2 shows the electrical results of p-type ZnO films with the variation of the dopants concentration deposited on glass substrate. All the films exhibit definitive p-type conductivity, indicating successful realization of p-type ZnO by dual acceptor doping of lithium and nitrogen. It can be seen that the resistivity, Hall mobility and carrier concentration of p-type ZnO films are almost the same with variation of dopant concentration. This may be due to the stress/strain and roughness of the films. From the Table 1, it is observed that the stress/strain and roughness of the film increases with the dopant concentration. In general, the electrical properties of thin films are related with their structural properties. At higher doping concentration of 8:8 (Li:N) mol%, the resistivity reaches a lowest value of 35.78 Ω cm. Thus, the Li and N content plays an important role in determining the p-type behaviour of (Li, N):ZnO films.

To verify the stability of p-type conductivity in (Li, N):ZnO, the electrical measurements are performed several times, and much the same results were obtained. The samples are preserved in ordinary silica gel desiccators. The p-type conductivity of (Li, N):ZnO films is very stable and do not revert to n-type even after 7 months. They have been maintaining more or less same electrical properties without any obvious degradation. Therefore the p-type behaviour is very much reproducible. Thus the self-compensation introduced by intrinsic defects in the films is suppressed due to dual acceptor doping.

3.3. Optical properties

The optical properties of (Li, N):ZnO thin films are determined from the transmission and reflection measurements in the wavelength range of 200–1200 nm. Fig. 3 shows the transmittance of

Table 2
Resistivity, carrier concentration and mobility of (Li, N):ZnO films.

Li (mol%)	N (mol%)	Resistivity (Ω cm)	Carrier concentration (cm^{-3})	Mobility $cm^2/(V\,s)$	*Carriertype*
2	2	325.52	8.00×10^{15}	2.40	p
4	4	60.09	5.20×10^{16}	2.00	p
6	6	49.30	8.34×10^{16}	1.52	p
8	8	35.78	8.20×10^{16}	2.13	p

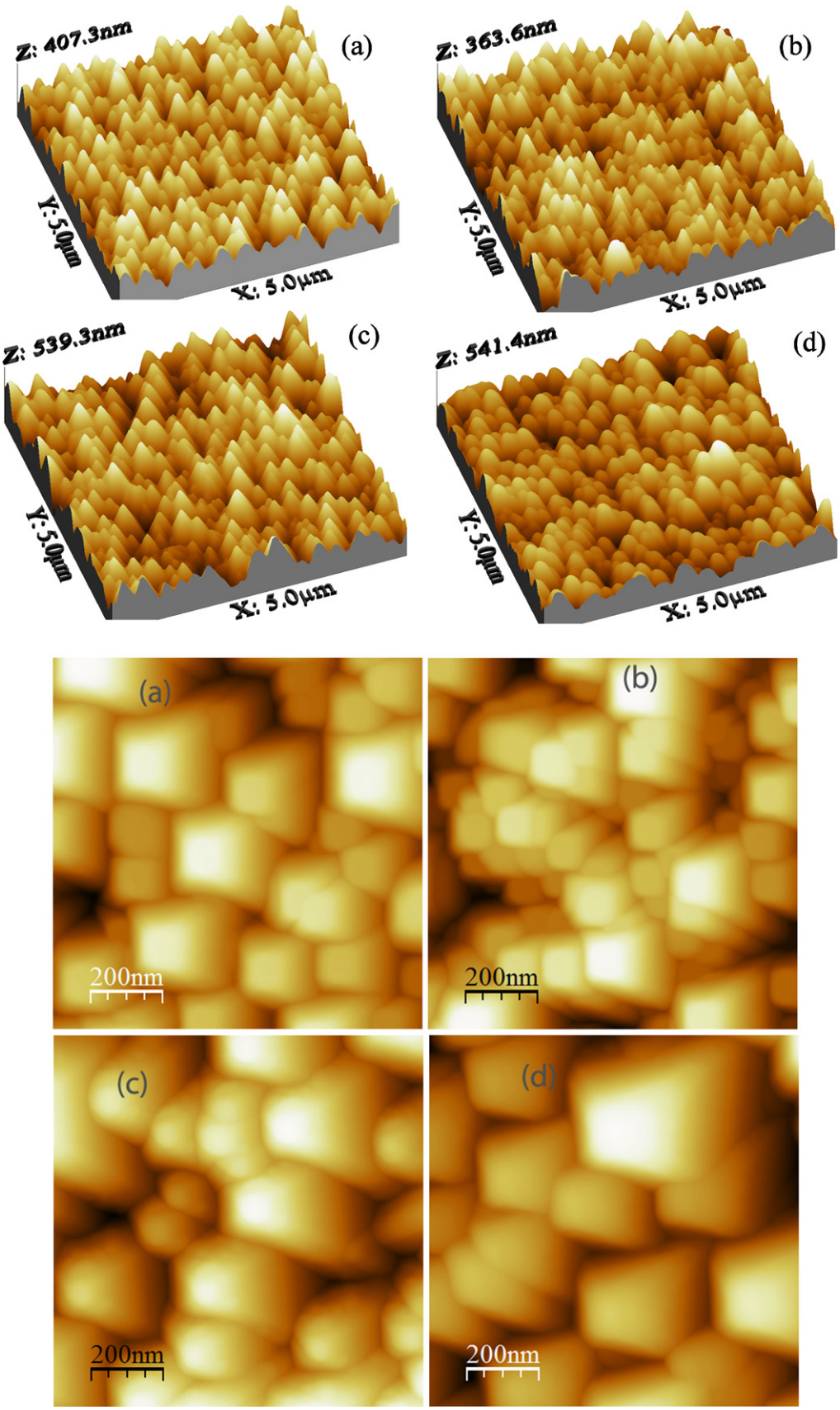

Fig. 2. AFM 3D and 2D images of (Li, N):ZnO films: (a) Li, N:2, 2 mol%, (b) Li, N:4, 4 mol% (c) Li, N:6, 6 mol% and (d) Li, N:8, 8 mol%.

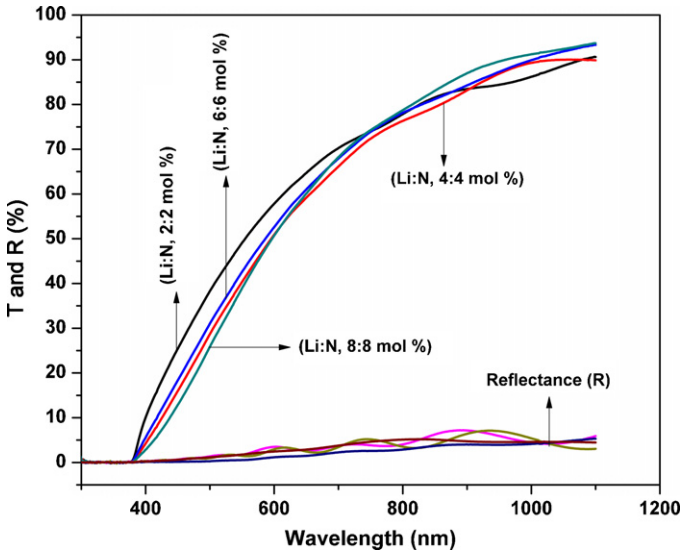

Fig. 3. Transmittance spectra of (Li, N):ZnO films.

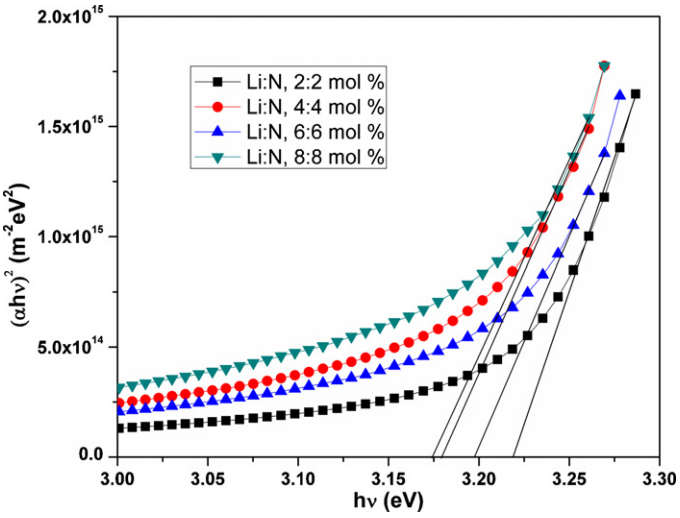

Fig. 4. $(\alpha h\nu)^2$ versus $h\nu$ spectra of (Li, N):ZnO thin films.

dual acceptor doped ZnO thin films prepared with different Li:N ratios (2:2, 4:4, 6:6 and 8:8 mol%). All the films are found to be transparent and it can be seen that the transmittance of the films decreases with increasing Li and N doping concentration. The optical transmittance of a film is known to depend strongly on its surface morphology. The rms surface roughness of the films increases with increase of dual acceptor doping concentration, which is evident from the AFM result. This indicates a reduction in surface smoothness leading to an increase in scattering loss. The transmission spectra do not show a sharp rise in absorption at absorption edge. This may be due to the perturbation of the parabolic density of the states at the band edges. It is known that the introduction of a high concentration of impurities in perfect semiconducting crystals causes a perturbation of the band structure with the result that the parabolic distribution of the states will be distributed and prolonged by a tail extending into the energy gap [19]. The XRD results shown that the stress and stain are higher in the (Li, N):ZnO films. There is a correlation between the stresses and the structural disorder in the films – the increase of the stress results in an increase of the Urbach band tail width [19]. It has also been observed that the distinct red shift of fundamental absorption edge for the films with higher Li and N concentration. The absorption coefficient α is calculated from the relation [20]:

$$T = (1 - R)\exp(-\alpha t) \quad (5)$$

where T is the transmittance, R is the reflectance and t is the film thickness. According to the band theory of solids, in a direct band gap semiconductor the relation between the absorption coefficient α and the energy of incident light $h\nu$ is given by [21]

$$\alpha h\nu = A\sqrt{h\nu - E_g} \quad (6)$$

in which A is a constant, E_g is the band gap energy. The direct band gap values of the films are determined by a plot of $(\alpha h\nu)^2$ as a function of the photon energy $h\nu$ as shown in Fig. 4. The band gaps of the films with different Li:N ratios of 2:2, 4:4, 6:6 and 8:8 mol% are 3.22, 3.19, 3.17 and 3.17 eV, respectively. It is observed that the band gap energy of Li, N-doped ZnO thin film decrease with increase of doping concentration. The band gap energy of Li, N-doped ZnO thin film is smaller than that of undoped ZnO thin film [22]. This can be probably due to the Li and N incorporation into ZnO films. This indicates a narrowing of the band gap of (Li, N):ZnO films for the p-type doping. According to previous report [23], the band gap narrowing of p-type ZnO can be understood from following effects: (i) the mergence of the impurity band with the valence or conduction band due to heavy acceptor agent doping [24], (ii) the conduction-band renormalization effects due to electron-ionized interaction and electron-ionized impurity interaction [25], and (iii) the change in ionicity [26].

Generally the optical band gap of n-type ZnO films shows a blueshift due to the Burstein-Moss effect, which is an energy band widening effect resulting from the raising of the Fermi level in the conduction band of degenerate semiconductors. However, the optical band gap of p-type ZnO films shows a redshift, which is related to Li and N doping. Since Li and N atoms are incorporated into the ZnO matrix, they would introduce strain in the films, which may cause the band gap to narrow down. It is well known fact that the band gap of a semiconductor is affected by the residual strain in the film. Earlier studies show that strain changes inter atomic spacing of semiconductors which affects the energy gap [27]. Optical band gap increases with increase in compressive strain along *c*-axis but decreases with increase in tensile strain [28,29]. This explains the decrease of E_g with the increase of tensile strain, when the Li:N doping concentration increases in ZnO.

Photoluminescence (PL) measurements were carried out with an excitation wavelength of 325 nm at room temperature. PL spectra are shown in Fig. 5. It is well known fact that there are mainly three photoluminescence peaks for ZnO. They are the near-band-edge (NBE) ultraviolet emission at about 380 nm, the green emission at about 510 nm and the red emission at about 650 nm, respectively [30]. From the PL spectra, it was observed that in all the cases there is a strong emission near UV, violet region and a weak defect-related deep level emission in visible regions. The major emission peaks observed near UV and violet are 3.36 eV (369 nm) and 3.12 eV (398 nm), respectively. The shoulder peak located at 3.36 eV for the (Li, N):ZnO film may be related to the Li and N impurities. This may be due to formation of Li_{Zn}–N_O complex acceptor [10,31]. We could not observe near UV peak in our previous work of pure ZnO thin films [32]. However the mechanism for near UV emission of (Li, N):ZnO films is not yet clear for room temperature PL.Wanga et al. [13] observed the emission peak at 3.10 eV in (Li, N):ZnO films at room temperature. The peak emission observed at 3.12 eV is very close to Wang et al. observation (3.10 eV). The peak emission at 3.12 eV may be ascribed to radiative electron transition from conduction band to intrinsic acceptor, such as vacancy Zn (V_{Zn}) [13]. The peak at 2.65 eV is blue emission, which originates from the defect emission of oxygen vacancies [33] and it is close to the reported value of 2.66 eV [34]. Fig. 5 also shows a broad

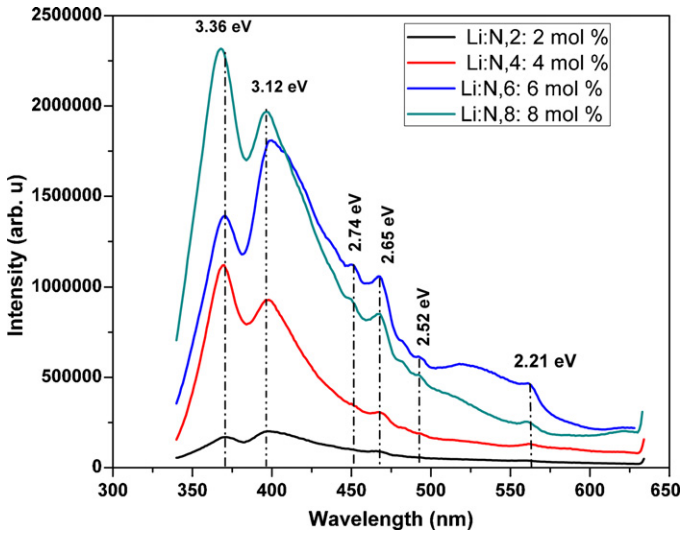

Fig. 5. PL spectra of (Li, N):ZnO thin films.

green-yellow emission with two peaks at 2.52 eV and another at 2.21 eV. Deep level emission in the vicinity of yellow-green region may be originated from the presence of oxygen vacancy [35]. These oxygen vacancies have been established a correlation with native defects. The 2.52 eV observed at nearly 2.44 eV in nitrogen and N-In co-doped ZnO samples by Bian et al. [36]. In addition to this, it is observed that the green band emission of the p-type ZnO film is much lower than that of the n-type ZnO film [32]. It is well known that such broad deep level emission is closely related to intrinsic defects such as Zn_i and V_O [37,38], which are believed to act as donor defects [39]. This indicates that the formation of such intrinsic defects is effectively suppressed by dual acceptor (Li, N) doping in ZnO thin films.

The chemical bonding states of N and Li in the films were examined by XPS analysis for the 8:8 mol% sample. N and Li dopants in the film are well detected and as shown in Fig. 6. The inner Zn 2p electron binding energy in the spectrum is ascribed to that of the zinc atom that exists in Zn–O. The strong O 1s peak is observed at 531.4 eV. It is broad and symmetric. The binding energy of Zn–O bonds in bulk is 530.6 eV [40]. It is also reported [40] that chemisorbed oxygen onto zinc has the binding energy of 531.8 eV. It is usually associated with the loosely bound oxygen (e.g. adsorbed O_2, –OH) chemisorbed on the surface or grain boundary of polycrystalline film [41,42]. Therefore, the peak around 531.4 eV is ascribed to Zn–O coordination in the complex. The broad N 1s peak is observed around 400 eV. In general, there are two basic possible bonds of N in ZnO: O–N and Zn–N, which can be regarded as N replacement of O and Zn, respectively [43]. No clear peaks are detected for O–N and Zn–N at 407.8 eV [44] and 395.8 eV [45], respectively. Therefore, we assigned N 1s peak around 400 eV for

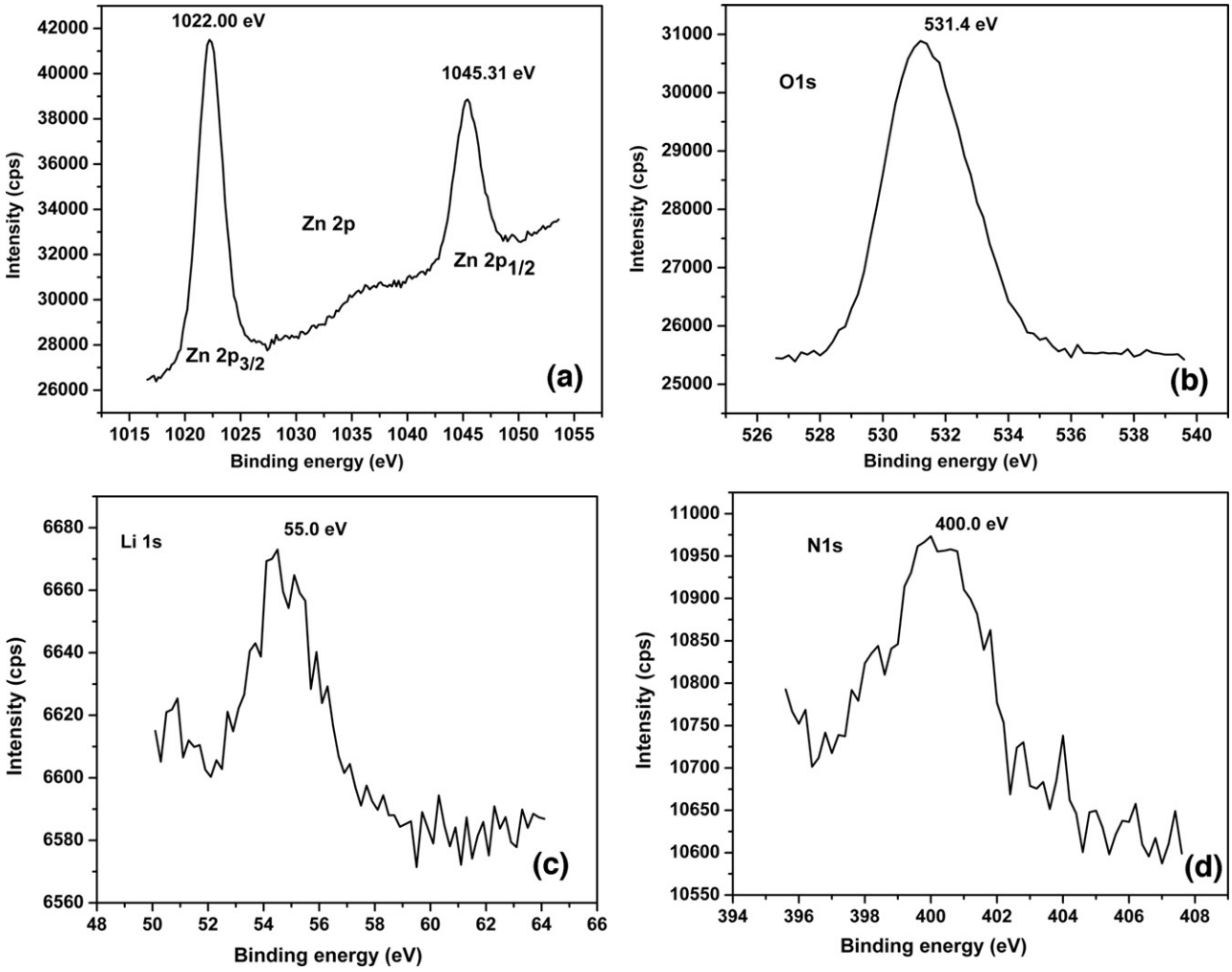

Fig. 6. XPS spectra of (Li, N):ZnO films (a) Zn 2p, (b) O 1s, (c) Li 1s and (d) N 1s.

N_O–Zn complex. The binding energy peak at 55.0 eV can be assigned to Li_{Zn}–O bonds. It is very close to the reported value 55.7 eV [46]. From the above discussion, it is clear that the Li and N incorporated into ZnO matrices. Therefore, XPS measurements substantiate p-type conduction in (Li, N):ZnO films. Since Li_{Zn} and N_O are acceptors, it is clear that the Li–N complex is an acceptor cluster and that p-type conductivity of the (Li, N):ZnO comes mainly from the contribution of the Li–N complex acceptors [10]. Recently, Wang et al. reported stable p-ZnO thin films using dual acceptors [47].

4. Conclusion

In summary, we have presented a promising Li–N dual acceptor doping method to realize p-type ZnO films via spray pyrolysis. The influence of concentration of Li–N on the structural, electrical, and optical properties of p-type ZnO:(Li, N) films were investigated in detail. It is found that (Li, N):ZnO films deposited on glass substrate show the preferential orientation of (002) plane. The surface roughness of the thin films, investigated by AFM, increased with increasing doping percentage. The Hall Effect measurements showed the p-type conductivity of on (Li, N):ZnO thin films. The lowest room-temperature resistivity was found to be 35.78 Ω cm for the concentration ratio of Li:N = 8:8 mol% with the hole concentration of 8.20×10^{16} cm^{-3}. The PL spectra of (Li, N):ZnO films showed a strong UV emission at room temperature. Furthermore, PL spectra showed low intensity in deep level transition, indicating a low density of native defects. This indicates that the formation of intrinsic defects is effectively suppressed by dual acceptor (Li, N) doping in ZnO thin films.

Acknowledgements

Authors are grateful to Dr. V. Ganesan and Dr. S.R. Barman for extending AFM and XPS facilities for carrying out this work at UGC-CSIR Consortium for Scientific Research, Indore, India. One of the authors (M.C.S. Kumar) is thankful to DST, Govt. of India for the financial support through SERC-Fast Track project for young Scientists.

References

[1] T. Yamamoto, H.K. Yoshida, Physica B 302–303 (2001) 155–162.
[2] G. Mandel, Phys. Rev. A 134 (1964) 1037–1048.
[3] C.H. Park, S.B. Zhang, S.U.H. Wei, Phys. Rev. B 66 (2002) 073202.
[4] M.G. Wardle, J.P. Goss, P.R. Briddon, Phys. Rev. B 71 (2005) 155205.
[5] E.C. Lee, Y.S. Kim, Y.G. Jin, K.J. Chang, Phys. Rev. B 64 (2001) 085120.
[6] T. Yamamoto, Thin Solid Films 420 (2002) 100–106.
[7] M. Joseph, H. Tabata, T. Kawai, Jpn. J. Appl. Phys. 38 (1999) L1205.
[8] Z.Z. Ye, Z.G. Fei, J.G. Lu, Z.H. Zhang, L.P. Zhu, B.H. Zhao, J.Y. Huang, J. Cryst. Growth 265 (2004) 127–132.
[9] J.M. Bian, X.M. Li, X.D. Gao, W.D. Yu, L.D. Chen, Appl. Phys. Lett. 84 (2004) 541–543.
[10] J.G. Lu, Y.Z. Zhang, Z.Z. Ye, L.P. Zhu, L. Wang, B.H. Zhao, Q.L. Liang, Appl. Phys. Lett. 88 (2006) 222114.
[11] A. Van der Drift, Philips Res. Rep. 22 (1967) 267–288.
[12] N. Fujimura, T. Nishihara, S. Goto, J. Cryst. Growth 130 (1993) 269–279.
[13] X.H. Wanga, B. Yao, D.Z. Shen, Z.Z. Zhang, B.H. Li, Z.P. Wei, Y.M. Lu, D.X. Zhao, J.Y. Zhang, X.W. Fan, L.X. Guan, C.X. Cong, Solid State Commun. 141 (2007) 600–604.
[14] T.M. Barnes, K. Olson, C.A. Wolden, Appl. Phys. Lett. 86 (2005) 112112.
[15] T. Prasada Rao, M.C. Santhoshkumar, Appl. Surf. Sci. 255 (2009) 4579–4584.
[16] N. Ashkenov, B.N. Mbenkum, C. Bundesmann, V. Riede, M. Lorenz, D. Spemann, E.M. Kaidashev, A. Kasic, M. Schubert, M. Grundmann, G. Wagner, H. Neumann, V. Darakchieva, H. Arwin, B. Monemar, J. Appl. Phys. 93 (2003) 126–133.
[17] J.F. Chang, C.C. Shen, M.H. Hon, Ceram. Int. 29 (2003) 245–250.
[18] M.K. Puchet, P.Y. Timbrell, R.N. Lamb, J. Vac. Sci. Technol. A 14 (1996) 2220–2230.
[19] D. Dimova-Malinovska, H. Nichev, O. Angelov, Phys. Stat. sol. 5 (10) (2008) 3353–3357.
[20] K.L. Chopra, Thin Film Phenomena, McGraw-Hill, New York, 1969, p. 734.
[21] D. Jiles, Introduction to the Electronic Properties of Materials, Chapman and Hall, New York, 1994, p. 180.
[22] T. Prasada Rao, M.C. Santhosh Kumar, S. Anbumozhi Angayarkanni, M. Ashok, J. Alloys Compd. 485 (2009) 413–417.
[23] Y.Z. Zhang, J.G. Lu, Z.Z. Ye, H.P. He, L.P. Zhu, B.H. Zhao, L. Wang, Appl. Surf. Sci. 254 (2008) 1993–1996.
[24] J.G. Lu, Z.Z. Ye, F. Zhuge, Y.J. Zeng, B.H. Zhao, L.P. Zhu, Appl. Phys. Lett. 85 (2004) 3134–3135.
[25] W. Walukiewicz, Phys. Rev. B 41 (1990) 10218–10220.
[26] G.D. Yuan, Z.Z. Ye, L.P. Zhu, Y.J. Zeng, J.Y. Huang, Q. Qian, J.G. Lu, Mater. Lett. 58 (2004) 3741–3744.
[27] J.I. pankove, Optical Processes in Semiconductors, Dover Publication, New York, 1971, p. 22.
[28] R. Ghosh, D. Basak, S. Fujihara, J. Appl. Phys. 96 (2004) 2689–2692.
[29] V. Srikant, D.R. Clarke, J. Appl. Phys. 81 (1997) 6357–6374.
[30] D.M. Bagnall, Y.F. Chen, M.Y. Shen, Z. Zhu, T. Goto, T. Yao, J. Cryst. Growth 184–185 (1998) 605–609.
[31] X.H. Wang, B. Yao, Z.P. Wei, D.Z. Shen, Z.Z. Zhang, B.H. Li, Y.M. Lu, D.X. Zhao, J.Y. Zhang, X.W. Fan, L.X. Guan, C.X. Cong, J. Phys. D: Appl. Phys. 39 (2006) 4578–4581.
[32] T. Prasada Rao, M.C. Santhosh Kumar, A. Safarulla, V. Ganesan, S.R. Barman, C. Sanjeeviraja, Physica B 405 (2010) 2226–2231.
[33] Y.H. Tong, Y.C. Liu, S.X. Lu, L. Dong, S.J. Chen, Z.Y. Xiao, J. Sol-Gel. Sci. Technol. 30 (2004) 157–161.
[34] X.Q. Wei, B.Y. Man, M. Liu, C.S. Xue, H.Z. Zhuang, C. Yang, Physica B 388 (2007) 145–152.
[35] E. Kaminska, A. Piotrowska, J. Kossut, R. Butkutė, W. Dobrowolski, R. Łukasiewicz, A. Barcz, R. Jakieła, E. Dynowska, E. Przeździecka, M. Aleszkiewicz, P. Wojnar, E. Kowalczyk, Phys. Status Solidi (C) 2 (2005) 1119–1124.
[36] J. Bian, W. Liu, J. Sun, H. Liang, J. Mater. Process. Technol. 184 (2007) 451–454.
[37] B. Lin, Z. Fu, Y. Jia, Appl. Phys. Lett. 79 (2001) 943–945.
[38] G.W. Tomlis, J.L. Routbort, T.O. Mason, J. Appl. Phys. 87 (2000) 117.
[39] S.B. Zhang, S.H. Wei, A. Zunger, Phys. Rev. B 63 (2001) 075205.
[40] S. Fujihara, C. Sasaki, T. Kimura, Appl. Surf. Sci. 180 (2001) 341–350.
[41] M. Chen, X. Wang, Y.H. Yu, Z.L. Pei, X.D. Bai, C. Sun, R.F. Huang, L.S. Wen, Appl. Surf. Sci. 158 (2000) 134–140.
[42] J.G. Ma, Y.C. Liu, R. Mu, J.Y. Zhang, Y.M. Lu, D.Z. Shen, X.W. Fan, J. Vac. Sci. Technol. B 22 (2004) 94–98.
[43] L.G. Wang, A. Zunger, Phys. Rev. Lett. 90 (2003) 256401.
[44] J.G. Lu, L.P. Zhu, Z.Z. Ye, F. Zhuge, Y.J. Zeng, B.H. Zhao, D.W. Ma, Appl. Surf. Sci. 245 (2005) 109–113.
[45] M. Futsuhara, K. Yoshioka, O. Takai, Thin Solid Films 322 (1998) 274–281.
[46] J.G. Lu, Y.Z. Zhang, Z.Z. Ye, Y.J. Zeng, H.P. He, L.P. Zhu, J.Y. Huang, L. Wang, J. Yuan, B.H. Zhao, X.H. Li, Appl. Phys. Lett. 89 (2006) 112113.
[47] X.H. Wang, B. Yao, C.X. Cong, Z.P. Wei, D.Z. Shen, Z.Z. Zhang, B.H. Li, Y.M. Lu, D.X. Zhao, J.Y. Zhang, X.W. Fan, Thin Solid Films 518 (2010) 3428–3431.